CORA Cork Open Research Archive
Cartlann Taighde Oscailte Chorcaí

Title	Effect of electrolyte concentration on anodic nanoporous layer growth for n-InP in aqueous KOH
Authors	Lynch, Robert P.;O'Dwyer, Colm;Buckley, D. Noel;Sutton, David;Newcomb, Simon B.
Publication date	2006-01-01
Original Citation	Lynch, R., O'Dwyer, C., Buckley, D. N., Sutton, D., Newcomb, S. B. (2006) 'Effect of Electrolyte Concentration on Anodic Nanoporous Layer Growth for n-InP in Aqueous KOH. ECS Transactions 2(5): 131-141; doi:10.1149/1.2204886
Type of publication	Article (peer-reviewed)
Link to publisher's version	http://ecst.ecsdl.org/content/2/5/131 - 10.1149/1.2204886
Rights	© The Electrochemical Society, Inc. 2006. All rights reserved. Except as provided under U.S. copyright law, this work may not be reproduced, resold, distributed, or modified without the express permission of The Electrochemical Society (ECS). The archival version of this work was published in Lynch, R., O'Dwyer, C., Buckley, D. N., Sutton, D., Newcomb, S. B. (2006) 'Effect of Electrolyte Concentration on Anodic Nanoporous Layer Growth for n-InP in Aqueous KOH. ECS Transactions 2(5): 131-141; doi:10.1149/1.2204886
Download date	2026-11-02 16:02:01
Item downloaded from	https://hdl.handle.net/10468/999

UCC
University College Cork, Ireland
Coláiste na hOllscoile Corcaigh

Effect of Electrolyte Concentration on Anodic Nanoporous Layer Growth for n-InP in Aqueous KOH

R. Lynch[a,b], C. O'Dwyer[c], D. N. Buckley[a,b], D. Sutton[a,d] and S. B. Newcomb[a,e]

[a] *Department of Physics, University of Limerick, Ireland*
[b] *Materials and Surface Science Institute, University of Limerick, Ireland*
[c] *Tyndall National Institute, University College Cork, Ireland*
[d] *present address: Department of Applied Science, Limerick Institute of Technology, Ireland*
[e] *present address: Glebe Scientific Ltd., Glebe Laboratories, Newport, Co. Tipperary, Ireland*

The surface morphology and sub-surface porous structure of (100) n-InP following anodization in 1 - 10 mol dm^{-3} aqueous KOH were studied using linear sweep voltammetry (LSV) in combination with scanning electron microscopy (SEM) and transmission electron microscopy (TEM). LSV of n-InP in 10 mol dm^{-3} KOH showed a single anodic current peak at 0.41 V. As the concentration of electrolyte was decreased, the peak increased in current density and charge and shifted to more positive potentials; eventually individual peaks were no longer discernable. Porous layers were observed in SEM cross-sections following linear potential sweeps and the porous layer thickness increased significantly with decreasing KOH concentration, reaching a maximum value at ~2.2 mol dm^{-3}. At concentrations less than 1.8 mol dm^{-3} the layer thickness decreased sharply, pore diameters became wider and pore walls became narrower until eventually, at 1.1 mol dm^{-2} or lower, no porous layers were observed. It was also observed that the pore width increased and the inter-pore spacing decreased with decreasing concentration. It is proposed that preferential pore propagation occurs along <111> directions, contrary to previous suggestions, and that the resulting nanoporous domains, initially formed, have triangular cross-sections when viewed in one of the {110} cleavage planes, 'dove-tail' cross-sections viewed in the orthogonal {110} cleavage plane and square profiles when viewed in the (100) plane of the electrode surface.

Introduction

Porosity in electrochemically etched semiconductors has been extensively investigated in the case of silicon and to a lesser extent in the case of III-V compounds such as GaAs (1,2) and InP (3-5). Anion type and concentration can play a significant role in affecting the pore growth and morphology (6,7). The depth of porous layers and their preferential crystallographic growth directions have been shown to be affected by the substrate type (8), orientation (9) and doping density (10).

In previous work by our group it has been observed that porous structures are obtained when InP is anodized in KOH at concentrations of 2 mol dm^{-3} or above (11).

Pores originating from pits in the surface create porous domains beneath a thin (~40 nm) dense near-surface layer and eventually these domains merge to create a continuous porous layer. This behaviour has been simulated numerically (12). However, at concentrations of 1 mol dm^{-3} or less, no porous layers were observed. This paper presents results of an investigation of the effect of KOH concentration on porous layer growth and presents additional data and analysis on preferential pore growth directions.

Experimental

The working electrode consisted of polished (100)-oriented monocrystalline sulfur-doped n-type indium phosphide (n-InP). An ohmic contact was made to the back of the InP sample and isolated electrically from the electrolyte by means of a suitable varnish. The electrode area was typically 0.5 cm^2. The InP had a carrier concentration of 3.4×10^{18} cm^{-3} and an etch pit density of less than 500 cm^{-2}. Anodization was carried out in aqueous KOH electrolytes in the concentration range 1-10 mol dm^{-3}. Each experiment involved a linear potential sweep (LPS) from 0.0 to 0.75 V (SCE) at 2.5 mV s^{-1}. A conventional three-electrode cell configuration was used employing a platinum counter electrode and saturated calomel reference electrode (SCE) to which all potentials were referenced. Prior to immersion in the electrolyte, the working electrode was dipped in an etchant (3:1:1 H_2SO_4:H_2O_2:H_2O) for 4 minutes and then rinsed in deionized water. All of the electrochemical experiments were carried out in the absence of light at room temperature.

A CH Instruments Model 650A Electrochemical Workstation interfaced to a Personal Computer (PC) was employed for cell parameter control and for data acquisition. Cleaved {011} cross-sections were examined using a JEOL JSM-6400F field emission scanning electron microscope (SEM) operating at 5 kV. Electron transparent sections for plan-view and cross-sectional transmission electron microscopic examination (TEM) were prepared using standard focused ion beam milling (FIB) procedures (13) in a FEI 200 FIB workstation. The TEM characterization was performed using a JEOL 2000FX TEM operating at 200 kV.

Results and Discussion

Figure 1 shows typical linear sweep voltammograms (LSVs) obtained for a series of concentrations. The curve at 10 mol dm^{-3} shows a single current peak at 0.41 V, typical of behaviour at higher concentrations. As the concentration is decreased, the peak increases both in current density and in area and shifts to more positive potentials. At 6 mol dm^{-3}, a single peak is observed (22 mA cm^{-2}, 0.43 V) but at 2 mol dm^{-3} the initial peak (~32 mA cm^{-2}, 0.53 V) is followed by additional partially resolved, broader peaks. With further decrease in concentration, individual peaks are eventually no longer discernable.

We have previously reported the formation of porous layers in the concentration range 2-5 mol dm^{-3} KOH. Figure 2 shows an SEM of an electrode cross-section following an LPS from 0.0 to 0.75 V in 10 mol dm^{-3} KOH. A ~0.8 μm porous layer is clearly visible. Similar layers were obtained at other concentrations in the range 2 – 10 mol dm^{-3}: an SEM cross-section following an LPS in 2 mol dm^{-3} KOH is shown in Figure 3. It can be seen that the layer is considerably thicker (~2.5 μm) than the layer obtained at 10 mol dm^{-3} (~0.8 μm). We observed a general increase in porous layer thickness with

decreasing concentration over this range (~2 – 10 mol dm^{-3}) in agreement with previous results (14) for the range 2 – 5 mol dm^{-3}.

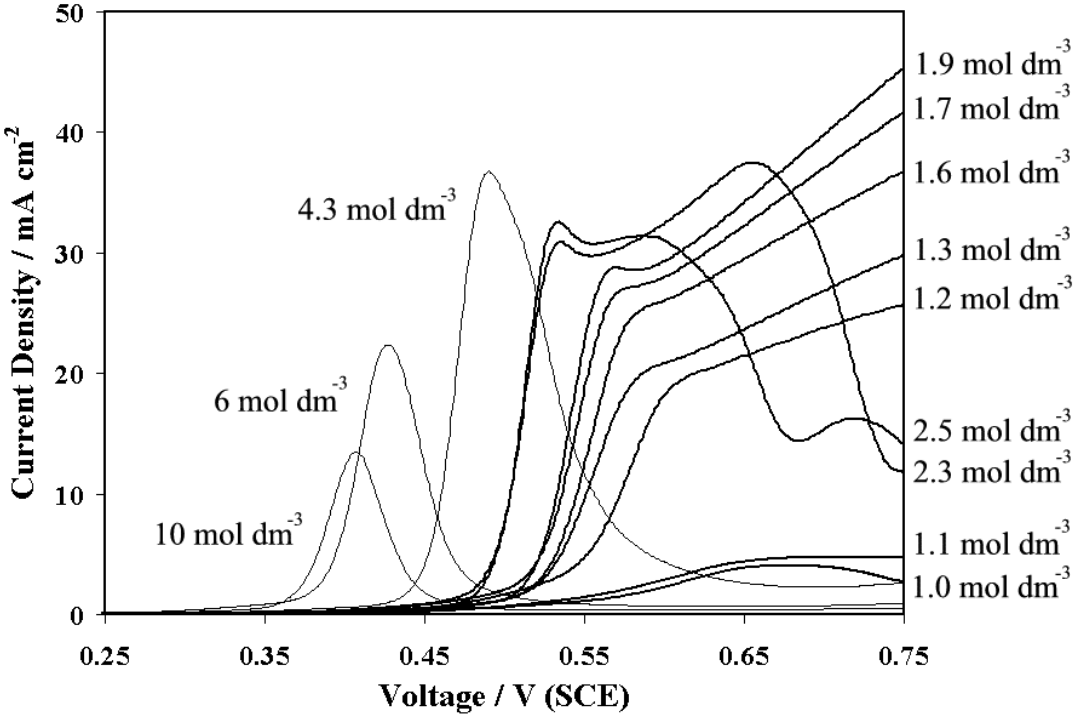


Figure 1. Linear sweep voltammograms from 0.0 to 0.75 V (SCE) at 2.5 mV s^{-1} for InP in various concentrations of KOH from 1 to 10 mol dm^{-3}.

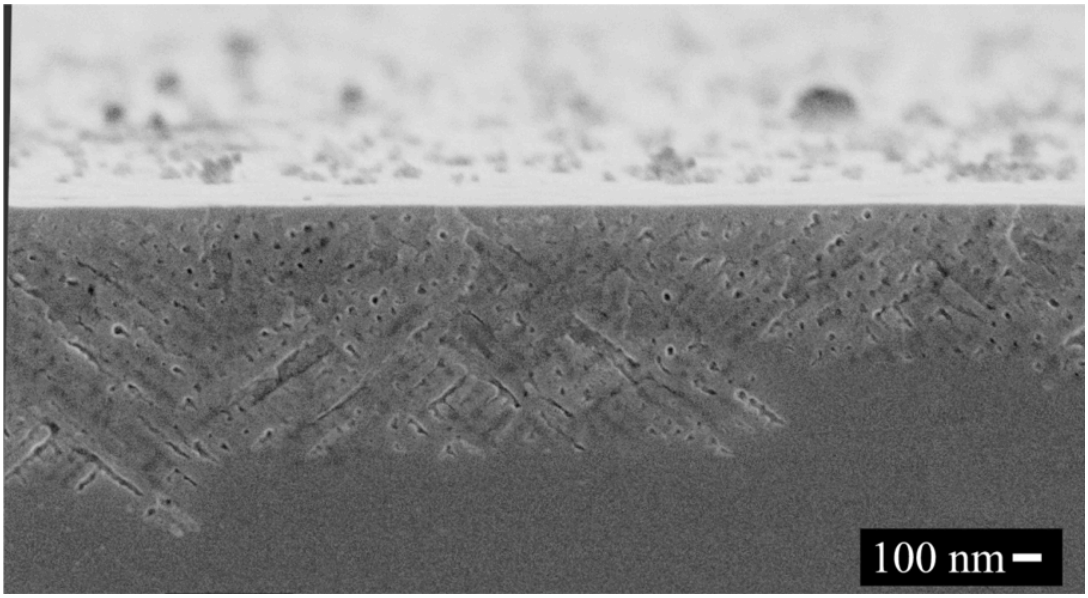


Figure 2. Cross-sectional SEM micrograph of an InP electrode following a LPS from 0.0 to 0.75 V (SCE) at 2.5 mV s^{-1} in 10 mol dm^{-3} KOH. The porous layer structure is clearly visible.

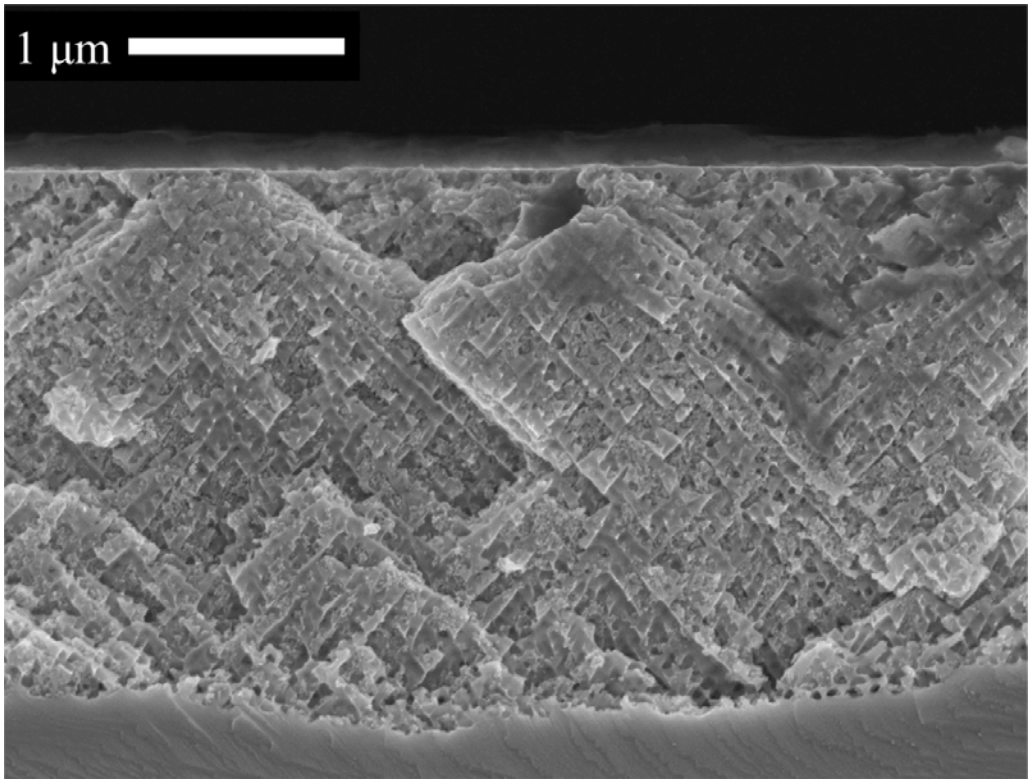


Figure 3. Cross-sectional SEM micrograph of an InP electrode following an LPS from 0.0 to 0.75 V (SCE) at 2.5 mV s^{-1} in 2 mol dm^{-3} KOH.

We also previously reported that no porous layer formation is observed in 1 mol dm^{-3} KOH. Figure 4 shows a series of SEM cross-sections of electrodes following LPSs at KOH concentrations ranging from 1.0 – 1.8 mol dm^{-3}. No porous layers are observed at 1 mol dm^{-3} (Figure 4a) or 1.1 mol dm^{-3} (Figure 4b). Figures 4c-f shows the transition to porous layer formation with increasing concentration. The layer obtained in 1.8 mol dm^{-3} KOH (Figure 4f) is clearly similar to layers obtained at higher concentrations although the dense near-surface layer observed at higher concentrations is not evident. However, the top (outer) surface of the layer is quite smooth and planar. At a concentration of 1.7 mol dm^{-3} the layer thickness is much less (~0.8 μm) and the surface appears to be rough. The pore size also appears to be somewhat larger. This trend to larger pore sizes and thinner layers continues as the concentration is decreased (Figure 4d and 4c, 1.6 mol dm^{-3} and 1.2 mol dm^{-3}) until eventually no porous layer formation is observed (Figure 4a 1.1 mol dm^{-3}).

At electrolyte concentrations between 1.8 mol dm^{-3} and 1.2 mol dm^{-3} the pore diameters are in the approximate range of 50 - 200 nm with pore walls of less than 10 nm in width and pores that eventually grow into each other. This is unlike the structures obtained at higher concentrations where inter-pore distances are greater and pore walls act as a barrier to the propagation of other pores. During the gradual transition from porous to non-porous etching, as the concentration is decreased, pore diameters become wider and pore walls become narrower until eventually anodization simply results in a rough surface that appears to become smoother at lower concentrations.

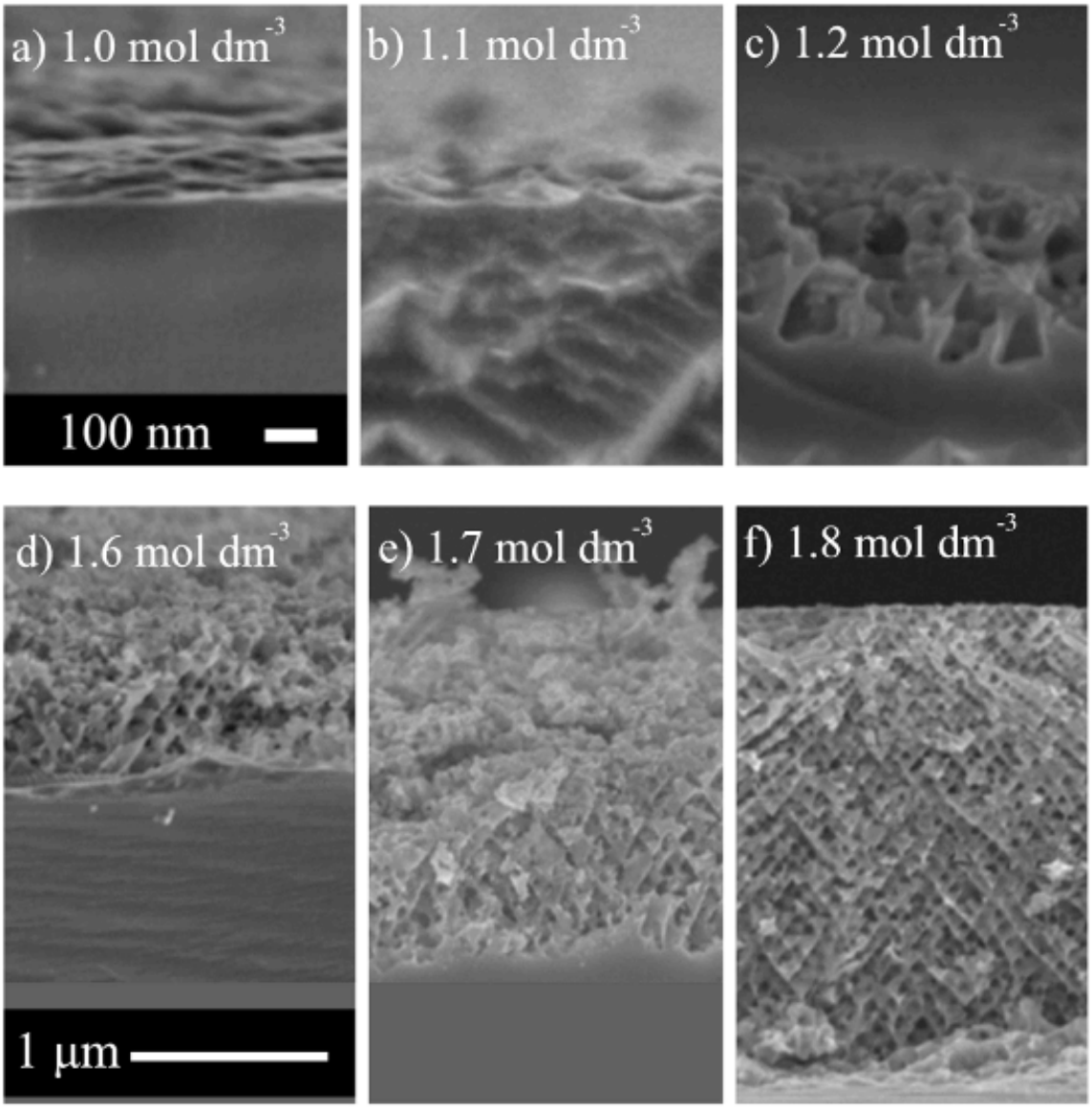


Figure 4. Cross-sectional SEM micrographs of InP electrodes following a LPS from 0.0 to 0.75 V (SCE) at 2.5 mV s^{-1} in KOH solutions of the concentrations shown.

The average thickness d_e of the porous layers was measured for each of the SEM micrographs in Figures 2, 3 and 4. The corresponding charge density Q was also estimated by integration of current density with respect to time in the LSVs. From Faraday's law, the (coulometric) thickness d_c of a compact InP layer equivalent to the quantity of InP oxidized by charge Q is given by

$$d_c = \frac{QV_{M,InP}}{nF} \qquad [1]$$

where $V_{M,InP}$ is the molar volume of InP, n is the number of electrons per formula unit of InP and F is the Faraday constant. Using a value of 30.31 cm^3 mol^{-1} for $V_{M,InP}$ (15) and assuming n = 8, a value of d_c was calculated in each case. Both the micrographic thickness d_e and the corresponding coulometric thickness d_c are plotted against KOH

concentration in Figure 5a. It is clear that the porous layer thickness increases significantly with decreasing concentration of KOH, reaching a maximum value at ~2.2 mol dm^{-3}. At concentrations less than this, the layer thickness decreases sharply. Although there appears to be considerable uncertainty in the value of d_e, possibly due to mechanical and/or chemical loss of some of the layer, it is clear from the d_c values that the layer thickness reaches a maximum value at ~2.2 mol dm^{-3}.

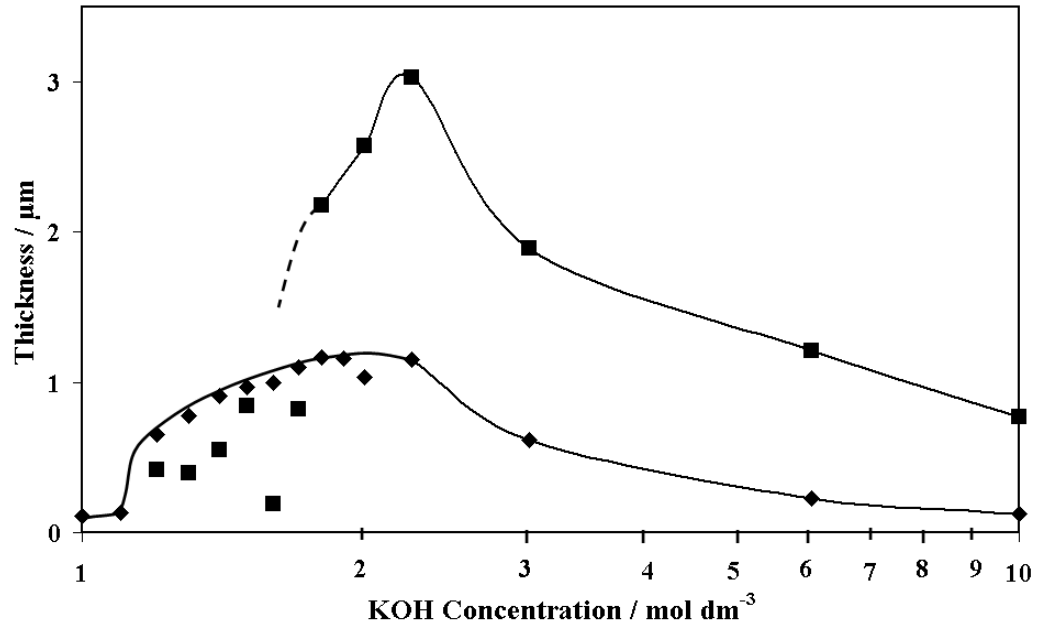
The porosity p is the ratio of the thickness d_c, which represents the quantity of InP removed, to the corresponding as-measured porous layer thickness d_e, i.e.

$$p = \frac{d_c}{d_e} \qquad [2]$$

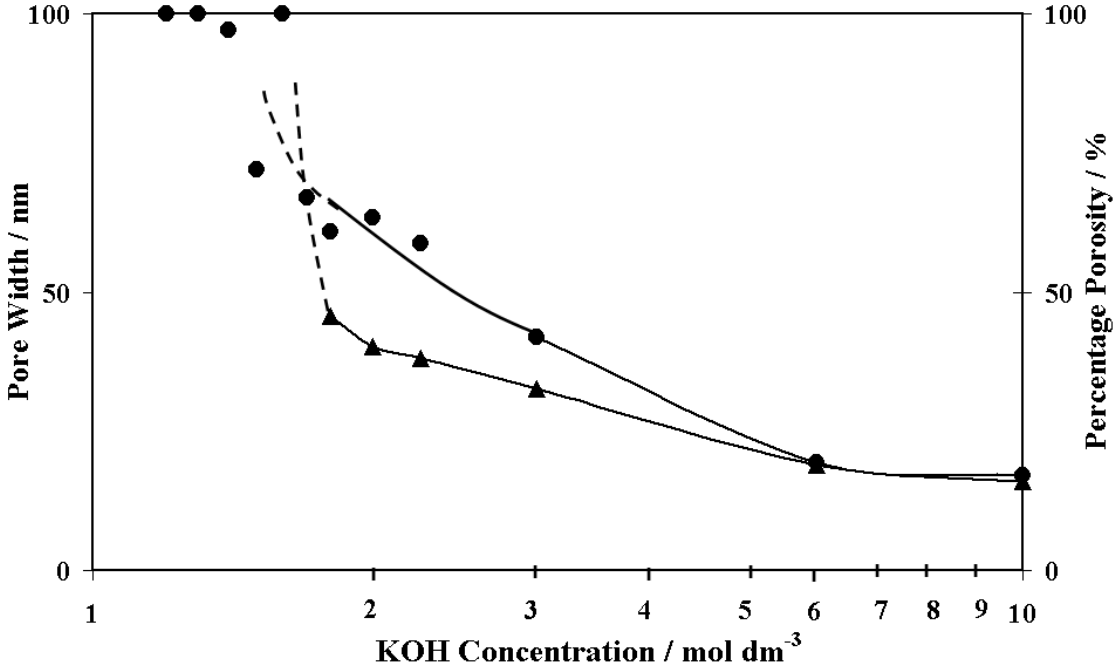
The porosity determined from the values of d_e and d_c in Figure 5a is plotted against concentration in Figure 5b. A gradual increase in porosity with decreasing electrolyte concentration, from ~18% at 10 mol dm^{-3} to ~40% at 2 mol dm^{-3}, is observed. At lower concentrations the estimated values are not reliable due to uncertainty in the value of d_e as mentioned above.

The average value of pore width for 15 randomly selected pores was also determined for each of the micrographs in Figures 2, 3 and 4. The resulting values are plotted against concentration in Figure 5b. It is observed that the pore width increases with decreasing concentration from ~17 nm at 10 mol dm^{-3} to ~62 nm at 2 mol dm^{-3}. Correspondingly, the inter-pore spacing decreases with decreasing concentration from ~40 nm at 10 mol dm^{-3} to ~ 15 nm at 2 mol dm^{-3}. This increase in pore width and corresponding decrease in inter-pore spacing is consistent with the observed increase in porosity with decreasing concentration. Below 2 mol dm^{-3}, the pore width continues to increase and the interpore spacing continues to decrease: measured values are imprecise because the interpore InP begins to disappear completely and individual pores are no longer well defined.

We have previously investigated (16) the earlier stages of anodic formation of porous InP in 5 mol dm^{-3} KOH and reported TEM evidence that clearly shows individual nanoporous domains which appear triangular in cross-section and square in plan view. The cross-sections also showed that the domains are separated from the surface by a ~40 nm, dense InP layer. TEM and AFM evidence showed that each domain develops from an individual surface pit which forms a channel through this near-surface layer and that eventually the domains merge to form a continuous nanoporous layer. We previously suggested that the porous domains have a square-based pyramidal shape arising from preferential pore propagation along the <100> directions. However, based on further investigation, we now propose that preferential pore propagation occurs along <111> directions and that the resulting nanoporous domains have a somewhat more complex shape as described below.

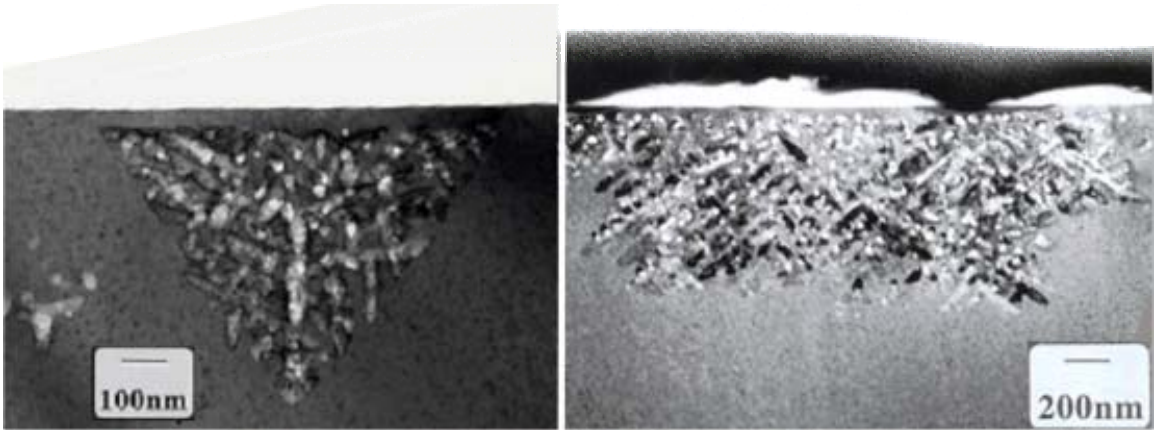


(a)



(b)

Figure 5. (a) Micrographically (■) and coulometrically (♦) determined thickness (de and dc, respectively) of the layers shown in Figures 2, 3 and 4 corresponding to the LSVs in Figure 1, plotted against KOH concentration. (b) Corresponding pore widths (●) measured from SEM micrographs and percentage porosity (▲) determined from the data in (a).



(a) **(b)**

Figure 6. TEM cross-sections of InP electrodes following LPSs at 2.5 mV s^{-1} in 5 mol dm^{-3}. The upper potential was 0.44 V (SCE) in the case of (a) and 0.48 V (SCE) in the case of (b). The plane of each micrograph is a {110}.

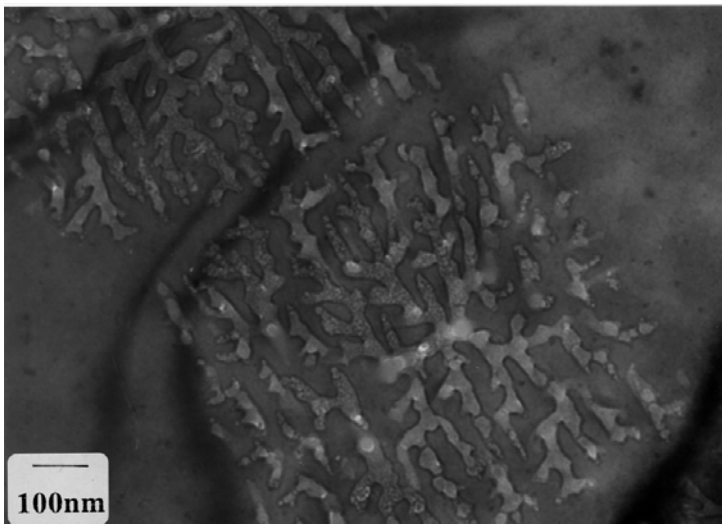
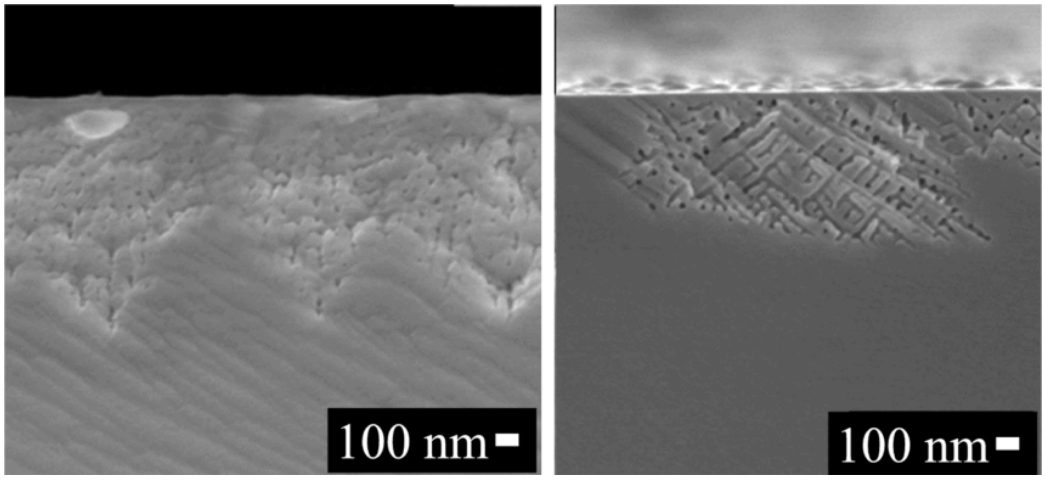


Figure 7. Plan view TEM image of a section through a porous InP layer ~100 nm below the surface of the electrode. Anodization conditions were the same as in Figure 6a. The plane of the micrograph is (100).

Figure 6a shows a TEM cross-section of an InP electrode after an LPS from 0.0 to 0.44 V (SCE) in 5 mol dm^{-3} KOH. This shows individual nanoporous regions having a triangular cross-section with the base of the triangle parallel to the InP surface. The nanoporous region is separated from the surface by a thin (~40 nm) non-porous near-surface layer as was observed for the more fully developed porous layer. Figure 6b shows another cross-section through an InP electrode following an LPS to 0.48 V in 5 mol dm^{-3} KOH. This shows what appears to be a quadrilateral section through a nanoporous domain that is overlapped on either side by similar but smaller domains. Figure 7 shows a TEM micrograph of a slice through the InP in the (100) plane, parallel to the electrode surface and ~100 nm below it, following anodization under the same conditions as in Figure 6a. A porous region with an approximately square outline is clearly visible.



(a) **(b)**

Figure 8. SEM cross-sections of InP electrodes following LPSs at 2.5 mV s^{-1} in 5 mol dm^{-3} KOH. The upper potential was 0.46 V (SCE) in the case of (a) and 0.45 V (SCE) in the case of (b). The planes of the micrographs are orthogonal {110} planes.

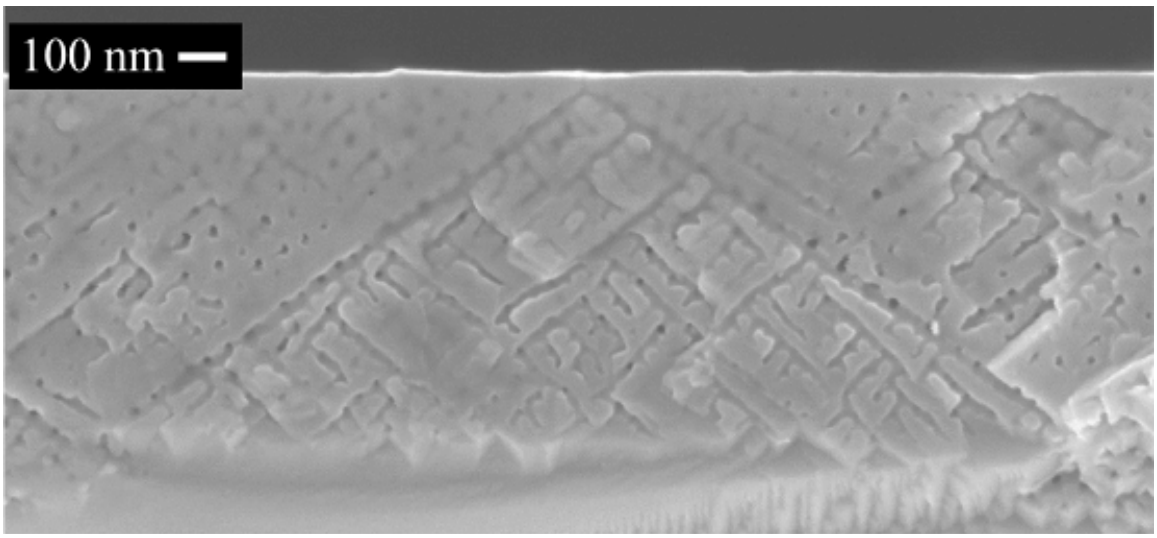


Figure 9. Cross-sectional SEM micrograph of InP following an LPS from 0.0 to 0.46 V (SCE) at 2.5 mV s^{-1} in 5 mol dm^{-3} KOH. Pore growth along <111> crystallographic directions is clearly visible.

Figure 8 shows similar cross-sections obtained by SEM. Figure 8a shows a cross-section through a layer obtained by a LPS to 0.46 V in 5 mol dm^{-3} KOH. It clearly shows overlapping domains with a triangular cross-section similar to Figure 6a. The SEM in Figure 8b shows a domain cross-section similar to that in Figure 6b.

Figure 9 shows the porous structure obtained following an LPS to 0.46 V in 5 mol dm^{-3} KOH. It can be seen that the pores grow along the {011} cleavage plane at 35° to the (100) electrode surface. This corresponds to pore growth along <111> directions. Careful examination of SEM and TEM cross-sections such as Figure 9 suggests that pores typically propagate along <111> directions. We will show elsewhere (17) that such directional growth of pores can lead to the formation of the type of porous domains

illustrated in Figure 10. These domains have triangular cross-sections when viewed in one of the {110} cleavage planes (corresponding to the images in Figures 6a and 8a), 'dove-tail' (trapezium shaped) cross-sections when viewed in the orthogonal {110} cleavage plane (corresponding to the images in Figures 6b and 8b) and square profiles when viewed in the (100) plane of the electrode surface (corresponding to the images in Figure 7).

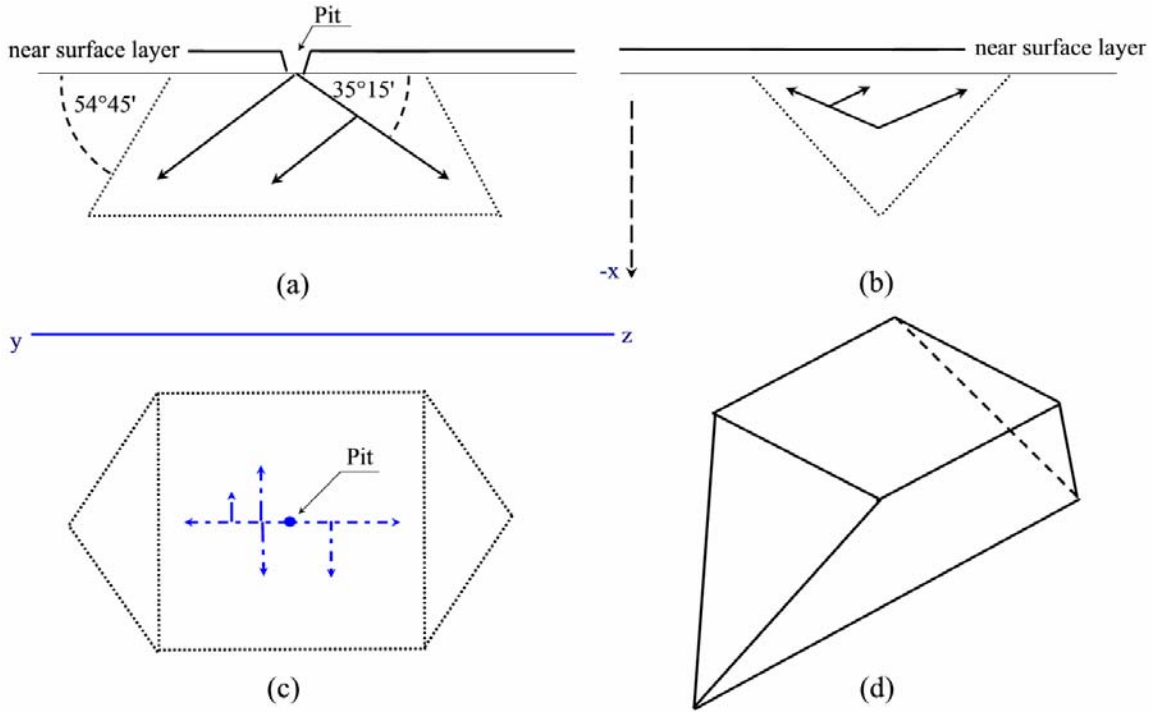


Figure 10. Technical drawing of porous domain showing (a, b) orthogonal {110} cleavage planes, (c) plan view in the plane of the electrode surface and (d) an isometric representation of its overall shape. The solid arrows indicate the <111> directions of pore growth and the broken arrows in (c) indicate their projection in the (100) plane.

Conclusions

LSVs of n-InP in 10 mol dm^{-3} KOH showed a single anodic current peak at 0.41 V. As the concentration of electrolyte was decreased, the peak increased both in current density and in charge and shifted to more positive potentials; eventually individual peaks were no longer discernable. Porous layers were observed in SEM cross-sections following LPSs and the porous layer thickness increased significantly with decreasing concentration of KOH, reaching a maximum value at ~2.2 mol dm^{-3}. At concentrations less than 1.8 mol dm^{-3} the layer thickness decreased sharply. No porous layers were observed at a concentration of 1.1 mol dm^{-2} or lower.

During the gradual transition from porous to non-porous etching as the concentration was decreased, pore diameters became wider and pore walls became narrower until eventually anodization simply resulted in a rough surface that appeared to become smoother at lower concentrations. A gradual increase in layer porosity with decreasing electrolyte concentration, from ~18% at 10 mol dm^{-3} to ~40% at 2 mol dm^{-3}, was observed. It was also observed that the pore width increased with decreasing

concentration from ~17 nm at 10 mol dm^{-3} to ~62 nm at 2 mol dm^{-3}. Correspondingly, the inter-pore spacing decreased with decreasing concentration from ~40 nm at 10 mol dm^{-3} to ~15 nm at 2 mol dm^{-3}.

It is proposed that preferential pore propagation occurs along <111> directions, contrary to previous suggestions, and that the resulting nanoporous domains initially formed have triangular cross-sections when viewed in one of the {110} cleavage planes, 'dove-tail' cross-sections when viewed in the orthogonal {110} cleavage plane and square profiles when viewed in the (100) plane of the electrode surface.

References

1. S. Langa, J. Carstensen, M. Christophersen, H. Föll, and I.M. Tiginyanu, *Appl. Phys. Lett.*, **78**, 1074 (2001).
2. G. Oskam, A. Natarajan, P.C. Searson and F.M. Ross, *Appl. Surf. Sci*., **119,** 160 (1997).
3. S. Langa, J. Carstensen, I.M. Tiginyanu, M. Christophersen and H. Föll, *Electrochem. Solid-State Lett.*, **4,** G50 (2001).
4. S. Langa, I.M. Tiginyanu, J. Carstensen, M. Christophersen and H. Föll, *Electrochem. Solid-State Lett.* **3**, 514 (2000).
5. R.L. Smith and S.D. Collins, *J. Appl. Phys*., **71**, 8 (1992).
6. P.Schmuki, J. Fraser, C. M. Vitus, M. J. Graham, H. S. Isaacs, *J. Electrochem. Soc.* **143,** 3316 (1996).
7. P. Schmuki, D. J. Lockwood, J. Fraser, M. J. Graham, H. S. Isaacs, *Mater. Res. Soc. Symp. Proc.,* **431,** 439 (1996).
8. M. Christopherson, J. Cartensen, A. Feuerhake and H. Föll, Mater. *Sci. Eng. B,* **69,** 70, 194 (2000).
9. S Rönnebeck, J. Carstensen, S. Ottow and H. Föll, Electrochem. *Solid-State Lett.,* **2,** 126 (1999).
10. P.Schmuki, L. E. Erickson, D. J. Lockwood, J. W. Fraser, G. Champion, H. J. Labbé, *Appl. Phys. Lett*., **72,** 1039 (1998).
11. D. N. Buckley, C. O'Dwyer, R. Lynch, *et al*., *Proceedings of the 41st State-of-the-Art Program on Compound Semiconductors*, PV 2004-05, p.103 (ECS, 2004).
12. R. Lynch, C. O'Dwyer, I. Clancy, *et al*., *Proceedings of the 41st State-of-the-Art Program on Compound Semiconductors*, PV 2004-05, p.85 (ECS, 2004).
13. L. A. Giannuzzi and F. A. Stevie, *Micron.*, **30**, 197 (1999).
14. C. O'Dwyer, D.N. Buckley, *et al. Proceedings of the 37th State-of-the-Art Program on Compound Semiconductors*, PV 2002-14 p. 259 (ECS, 2002).
15. CRC Handbook of Chemistry and Physics 86th ed.: *Physical Constants of Inorganic Compounds,* p. 4-65, D. R. Lide, Editor-in-Chief, CRC Press, New York (2005).
16. C. O'Dwyer, D.N. Buckley, *et al. Proceedings of the 38th State-of-the-Art Program on Compound Semiconductors*, PV 2003-04 p. 63 (ECS, 2003).
17. R. Lynch, C. O'Dwyer, D. N. Buckley, D. Sutton and S. B. Newcomb, *to be published.*